Bioelectrochemistry 98 (2014) 87–93

Contents lists available at ScienceDirect

Bioelectrochemistry

journal homepage: www.elsevier.com/locate/bioelechem

Design synthesis of polypyrrole–Co_3O_4 hybrid material for the direct electrochemistry of Hemoglobin and Glucose Oxidase

Sheying Dong [a,*], Lei Peng [a], Dan Liu [a], Qiangxu Yang [a], Tinglin Huang [b]

[a] College of Sciences, Xi'an University of Architecture and Technology, Xi'an, 710055, China
[b] School of Environmental and Municipal Engineering, Xi'an University of Architecture and Technology, Xi'an 710055, China

ARTICLE INFO

Article history:
Received 22 December 2013
Received in revised form 1 April 2014
Accepted 1 April 2014
Available online 13 April 2014

Keywords:
Polypyrrole–Co_3O_4
Hybrid material
Protein/enzyme
Direct electron transfer

ABSTRACT

We designed and synthesized a novel organic–inorganic hybrid material polypyrrole–Co_3O_4 (Ppy–Co_3O_4), then mixed it with ionic liquid (IL) to form stable composite films for the immobilization of Hemoglobin (Hb) and Glucose Oxidase (GOD). The combination of Ppy and Co_3O_4 as well as IL created a platform with exceptional characteristics, and the content of Ppy had an effect on the direct electron transfer (DET) of Hb/GOD. Notably, when weight percentage of pyrrole monomer was 20%, the heterogenous electron transfer rate constant (k_s) for Hb and GOD was estimated to be 1.71 s^{-1} and 1.67 s^{-1}, respectively. In the meantime, electrochemical and spectroscopic measurements showed that Hb/GOD remained their bioactivity, and achieved fast electron transfer on the Ppy–Co_3O_4/IL composite film modified electrode. Furthermore, the Ppy–Co_3O_4/IL/Hb composite film modified electrode was used as a biosensor, and exhibited a long linear range and lower detection limit to H_2O_2. The apparent Michaelis–Menten constant (K_m) was found to be 0.53 mM. The sensing design based on the Ppy–Co_3O_4 hybrid material was demonstrated to be effective and promising in developing protein and enzyme biosensors.

1. Introduction

Studies on the DET of redox proteins/enzymes not only help to establish a desirable model for studying the redox mechanism of proteins and enzymes in biological systems [1], but also can exploit biofuel cells [2], electrochemical biosensors [3,4], and bioreactor devices [5]. Unfortunately, it's difficult to realize DET between conventional electrodes and proteins or enzymes because of their denaturation on conventional electrode and deeply buried electroactive centers. Thus, various nanomaterials, such as metal nanoparticles [6], metal oxides [7], carbon nanomaterial [8] and their composite [9,10] have been applied to promote the electron transfer of Hb/GOD. However, most references focused on the immobilization of one kind of protein or enzyme by different nanomaterials. To the best of our knowledge, there are few reports on the immobilization of two kinds of proteins or enzymes by exploiting a variety of functions of composite materials.

Co_3O_4 is an important transition metal oxide with intriguing electronic, electrochemical and electrocatalytic properties, and its normal spinel crystal structure is favorable for electron transportation between Co^{2+} and Co^{3+} ions. Currently, Co_3O_4 and Co_3O_4-based composite have exhibited great potential application in supercapacitors [11], batteries [12], heterogeneous catalysts [13] and electrochemical sensors [14,15]. Especially, Co_3O_4 has been shown to be an excellent sensing material for constructing various sensors due to its superior capabilities in terms of response range, detection limit, stability and anti-interference property [16,17].

Alternatively, Ppy, one representative conducting polymer with attractive features for their unique conjugated π-electron system, such as good environmental stability, high electrical conductivity, good biocompatibility as well as ease of preparation, is a suitable matrix for the immobilization of various redox proteins or enzymes on electrodes [18,19]. It is expected that a novel organic–inorganic composite structure Ppy–Co_3O_4 will provide a conductive network for efficient charge transfer as well as more binding sites for the protein/enzyme. In addition, previous researches demonstrated that IL was a kind of ideal matrix that could disperse the nanomaterials into the modified layers to improve the stability and promote the electrocatalysis of protein/enzyme [20,21].

In this work, we proposed a procedure to synthesize Ppy–Co_3O_4 hybrid nanocomposite. Meantime, the material was characterized by scanning electron microscopy (SEM) and used as supports for Hb/GOD immobilization with good dispersion effect and excellent conductivity IL. Furthermore, the DET of the Ppy–Co_3O_4/IL/GOD and Ppy–Co_3O_4/IL/Hb composite film modified carbon paste electrode (CPE) was investigated, respectively. In addition, we have also evaluated the resultant Ppy–Co_3O_4/IL/Hb composite film in H_2O_2 biosensing as the sensitive and accurate H_2O_2 detection.

* Corresponding author. Tel.: +86 29 82201203; fax: +86 29 82205332.
E-mail address: dongsyy@126.com (S. Dong).

http://dx.doi.org/10.1016/j.bioelechem.2014.04.001
1567-5394/

2. Experimental section

2.1. Reagents

Hemoglobin (Hb, MW 64,500) and Glucose Oxidase (GOD, MW 150,000) were both purchased from Sigma Chemical Co., and [BMIm] BF_4 IL was purchased from Hangzhou Chemer Chemical Limited Company. High purity graphite powder, dodecylsulfate (SDS), ethylene glycol (EG), polyethylene glycol 400 (PEG400) and Pyrrole monomer were obtained from China National Medicine Corporation. $K_3Fe(CN)_6$, $K_4Fe(CN)_6$, KCl, K_2HPO_4, KH_2PO_4, Na_2CH_3COOH, $FeCl_3 \cdot 6H_2O$, $CoCl_2 \cdot 6H_2O$, H_2O_2 (30%) and liquid paraffin were obtained from Xi'an Chemical Reagent Corporation. All other chemicals were of analytical reagent grade and used without further purification. All solutions were made up with twice-distilled water.

2.2. Apparatus

The microstructures of Co_3O_4 and Ppy–Co_3O_4 were analyzed by scanning electron microscopy (SEM; JEOL JSM-6360, Japan). UV–vis spectra were recorded on a Nicolet Evolution 300 spectrophotometer in 0.1 M phosphate buffer solutions. Consolidate the first paragraph and second paragraph in the Apparatus part.

(PBS) and the IR spectra (KBr) were recorded on an IR-spectrometer FTIR-8400S Shimadzu at room temperature. The powder X-ray diffraction (XRD) patterns were recorded with a Rigaku Dmax-rA X-ray diffractometer using Cu Kα radiation.

All electrochemical measurement was carried out with a CHI660d electrochemical workstation (Shanghai Chenhua Co.) controlled by a microcomputer with CHI660 software. A three electrode system was used, where an Ag/AgCl electrode (3.0 M KCl, Shanghai Ruosull Tech. Co.) served as the reference electrode, a platinum wire electrode as the auxiliary electrode and a modified CPE as the working electrode. Amperometric experiments were performed in a constant stirred cell with the successive addition of H_2O_2 into 20.0 mL supporting electrolyte, while the electrode potential was set at −350 mV for H_2O_2 vs. RE (Ag/AgCl). The transient background current was allowed to decay to a steady-state value before adding analytes. Stock solutions of H_2O_2 were freshly prepared from 30% H_2O_2 solution.

All experimental solutions were deoxygenated by purging them with highly pure nitrogen for 30 min and maintained under nitrogen atmosphere during measurements. AC impedance experiments were carried out in 5.0 mM $K_3Fe(CN)_6/K_4Fe(CN)_6$ (1:1) solution containing 0.1 M KCl, while the applied perturbation amplitude was 0.005 V, the frequencies swept from 10^5 to 10^{-2} Hz, the number of points per frequency decade was 12 and the initial potential was 0.20 V vs. RE (Ag/AgCl).

2.3. The preparation of Co_3O_4 and Ppy–Co_3O_4

Co_3O_4 was synthesized according to the procedure reported previously with a little modification [22]. Following that, Ppy–Co_3O_4 was prepared by oxidative polymerization of pyrrole. First, the obtained 0.04 g Co_3O_4 particles were dispersed in 50 mL of aqueous solution containing 0.02 g SDS under the ultrasonic condition for about 5 min, then vigorous stirring for about 3 h at room temperature. The solution was then put into refrigerator for about 5 min. Next, defined amount of pyrrole monomer and 5 mL of $FeCl_3$ aqueous solution in a mole ratio of 1:1 was subsequently introduced to the above solution. The polymerization reaction continued for 4 h under magnetic stirring. Finally, the resulting hybrid particles were centrifuged and washed with water and ethanol several times, dried at 60 °C overnight to obtain the Ppy–Co_3O_4 composite. The products were marked as m Ppy–Co_3O_4 (m, mass content of pyrrole in the hybrid material).

2.4. Preparation of the modified electrodes

CPE was prepared as described previously [23]. The preparation of Hb/GOD modified electrode: 5 mg of Ppy–Co_3O_4 and 10 μL brominated 1-methyl-3-butyl imidazole ionic liquid (BmimBr IL) were dispersed into 1 mL of 0.1 M pH 7.0 PBS under sonication. Then 5 μL of the above suspension was casted onto the surface of a freshly polished CPE to obtain Ppy–Co_3O_4/IL-CPE, which was dried at room temperature to form a stable film. Finally, Ppy–Co_3O_4/IL/Hb-CPE and Ppy–Co_3O_4/IL/GOD-CPE were prepared by casting 5 μL Hb solution (5 mg/mL) or 5 μL GOD solution (10 mg/mL) onto the Ppy–Co_3O_4/IL-CPE. The Hb/GOD electrode was dried at 4 °C in a refrigerator and then rinsed twice or thrice with doubly distilled water to remove the unadsorbed protein/enzyme molecules.

3. Results and discussion

3.1. The designed synthesis and characterization of Ppy–Co_3O_4

The stepwise construction of Ppy–Co_3O_4 is represented in Scheme 1. One novel aspect of this work lies in the designed synthesis of Ppy–Co_3O_4. Firstly, the Co_3O_4 was prepared via the reactions between $CoCl_2$ and EG under solvothermal condition. Following, the SDS molecules were used to protect Co_3O_4 particles from forming enlarged particles, and made them surrounded by negative charges. After pyrrole monomer was added, in situ oxidative polymerization of pyrrole monomer occurred with the introduction of $FeCl_3$, in which the polymer chains acquired positive charges. Ppy layer with electropositive was gradually deposited on the surface of Co_3O_4 particles due to electrostatic interactions.

The typical SEM images of Co_3O_4 and Ppy–Co_3O_4 materials are shown in Fig. 1. Obviously, the bare Co_3O_4 is similar to spherical shape, and seems to consist of many interweaving nanosheets of loose structure. When Ppy layer was gradually deposited on the surface, both the edge of Co_3O_4 and the nanostructure of Ppy were clearly observable in the higher magnification images of insert in Fig. 1C. Ppy–Co_3O_4 hybrid material not only maintained its loose structure but also was partly surrounded by Ppy. From the surface morphologies of different contents of Ppy, it was interestingly found that the decorated Ppy had an obvious increase with increasing pyrrole monomer content. However, the obvious rough surface was observed with further increase of pyrrole monomer content to 40% in the inset of Fig. 1D. Thus, the SEM results support the formation of the Ppy–Co_3O_4 hybrid material. In addition, the XRD pattern of Co_3O_4 showed a well resolved diffraction (see Fig. 1E), which can be assigned to face-centered cubic Co_3O_4 phase in good agreement with standard JCPDS card number: 43-1003. No peaks from other phases are found, suggesting that the product is completely transformed into Co_3O_4 after annealing.

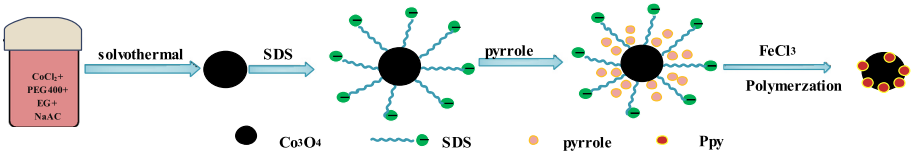

Scheme 1. Schematic illustration of the synthesis process of Ppy–Co_3O_4.

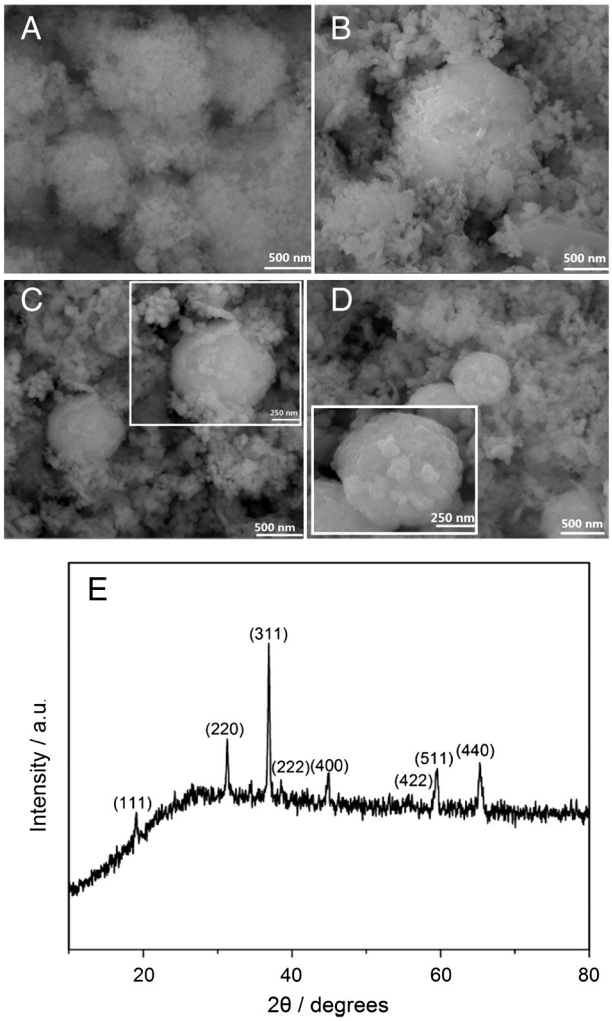

Fig. 1. SEM images of (A) Co_3O_4, (B) 5% Ppy–Co_3O_4, (C) 20% Ppy–Co_3O_4, (D) 40% Ppy–Co_3O_4. The insets of C and D are the high magnification SEM image themselves. XRD pattern (E) of Co_3O_4.

3.2. Spectroscopic characterization results

It is well known the position of the absorption band of proteins/enzymes in the UV–vis spectroscopy provides information about possible denaturation of proteins, especially conformational change [24]. Fig. 2 showed the UV–vis spectra of different modified solutions. The mixture of 5 mg/mL Ppy–Co_3O_4, 10 μL/mL IL and 5 mg/mL Hb or 10 mg/mL, the GOD with the volume ration of 1:1 was diluted with PBS. And then the resulting solution was in a refrigerator before analyzing on a UV–visible spectrophotometer from 250 to 550 nm. It was obvious that Hb (Fig. 2A-b) and GOD (Fig. 2B-b) in Ppy–Co_3O_4/IL nanocomposite film kept nearly the same Soret band as native Hb (Fig. 2A-a) and GOD (Fig. 2B-a) film, indicating that Hb and GOD in the composite film maintained their natural state well. At the same time, the characteristic infrared adsorption bands of amide I (1700–1600 cm^{-1}) and amide II (1600–1500 cm^{-1}) can provide detailed information on the secondary structure of polypeptide chain [25]. Thus, FT-IR spectroscopy was also employed to investigate the structural variations of Hb and GOD immobilized into the Ppy–Co_3O_4/IL composite film. The process occurs sequentially with Hb/GOD immobilized on a piece of glass surface, dried and then coated with a suspension of Ppy–Co_3O_4/IL. The glass was in a refrigerator and then was analyzed on an IR-spectrometer. As shown in Fig. 3, the spectra of free Hb (Fig. 3A-a) and GOD (Fig. 3B-a) were similar to those of Hb (Fig. 3A-b) and GOD (Fig. 3B-b) immobilized on the Ppy–Co_3O_4/IL composite film, which confirmed that the secondary structure of the Hb/GOD almost retained its original structure [7]. These studies indicated that the Ppy–Co_3O_4/IL composite film could provide a promising matrix for the further study of DET of Hb/GOD.

3.3. Electrochemical impedance spectroscopy (EIS)

To study the role of each component in the composite, the electron transfer capability of the modified electrodes was investigated by EIS in Fig. 4. The high electron transfer resistance (R_{et}) of CPE (curve g) indicated an inefficient electron transfer process at the surface of CPE, while the Co_3O_4 and IL contributed to a slight decrease of R_{et} of Co_3O_4–CPE (curve f) and IL-CPE (curve d). As shown in inset B of Fig. 4, when Ppy–Co_3O_4 nanocomposites were coated on the CPE, it was found that the R_{et} further decreased with the increase of weight percentage of pyrrole monomer, suggesting Ppy had been successfully introduced into Co_3O_4, and Ppy deposited on Co_3O_4 played the role of electron channel. For Ppy–Co_3O_4/IL-CPE (curve a), a smaller R_{et} was observed, due to the synergistic effect of IL and Ppy–Co_3O_4 which facilitated the conductivity of hybrid material. However, the presence of Hb/GOD led to the increase of the impedance of the Ppy–Co_3O_4/IL/Hb-CPE (curve c) and Ppy–Co_3O_4/IL/GOD-CPE (curve e), indicating that Hb/GOD was successfully immobilized on the Ppy–Co_3O_4/IL composite film.

3.4. Direct electrochemistry of Hb and GOD

The electrochemical behaviors of different modified electrodes were examined by cyclic voltammetry (CV) in 0.1 M PBS (pH 7.0) at a scan rate of 0.1 V s^{-1} and the results were shown in Fig. 5. No obvious redox peaks were observed for the Ppy–Co_3O_4/IL/CPE, suggesting that Ppy–Co_3O_4 and IL were electro-inactive in both potential windows. Both Co_3O_4/IL/Hb-CPE (Fig. 5A-b) and Co_3O_4/IL/GOD-CPE (Fig. 5B-b) gave a couple of ill-defined and poor reversible redox peaks, indicating

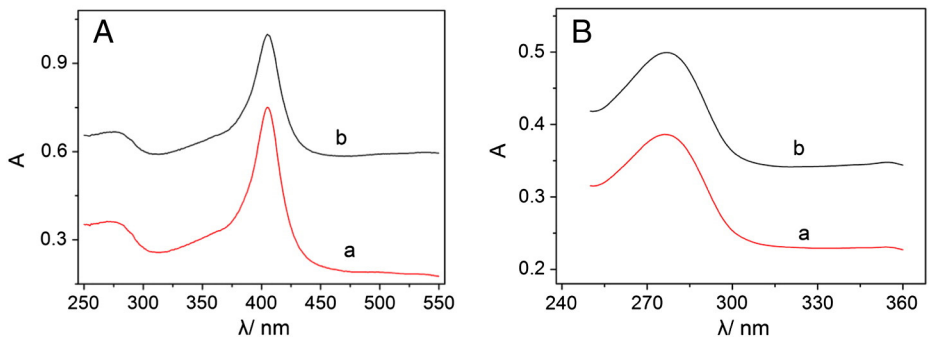

Fig. 2. UV–vis spectra of different solutions (0.1 M pH 7.0 PBS) containing (A) Hb (a) and Ppy–Co_3O_4/IL/Hb (b), and (B) GOD (a) and Ppy–Co_3O_4/IL/GOD (b).

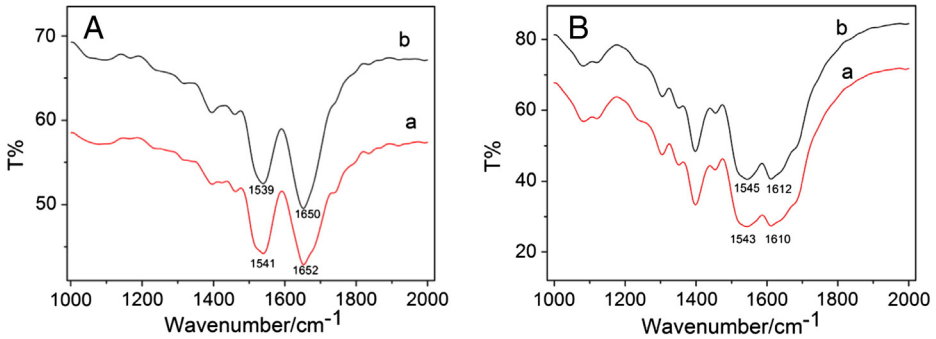

Fig. 3. FTIR spectra of (A) Hb (a) and Ppy–Co_3O_4/IL/Hb composite (b), and (B) GOD (a) and Ppy–Co_3O_4/IL/GOD composite (b).

a slow electron transfer process. However, the electrochemical performances of Ppy–Co_3O_4/IL/Hb-CPE and Ppy–Co_3O_4/IL/GOD-CPE were also regulated by the control of weight percentage of pyrrole monomer. For 5% Ppy–Co_3O_4/IL/Hb-CPE (Fig. 5A-c) and 5% Ppy–Co_3O_4/IL/GOD-CPE (Fig. 5B-c), their peak current values were increased slightly and a smaller peak-to-peak separation was obtained. As shown in Fig. 5A-d and Fig. 5B-d, the responses at 20% Ppy–Co_3O_4/IL/Hb-CPE and 20% Ppy–Co_3O_4/IL/GOD-CPE were apparently enhanced and their reversibilities were improved significantly. The anodic and cathodic peak potentials were located at −0.276 V and −0.364 V with the formal potential

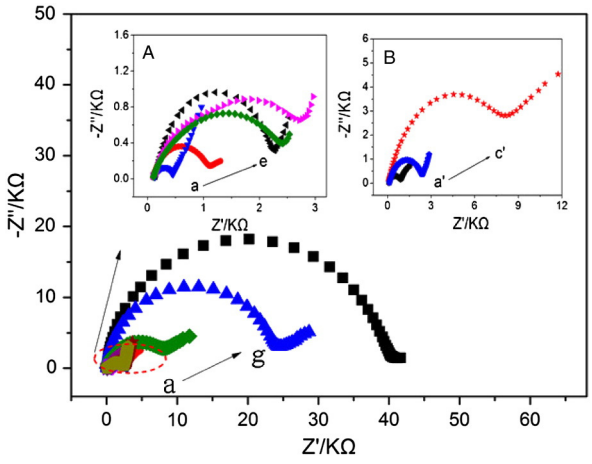

Fig. 4. EIS of different electrodes in 5.0 mM $K_3Fe(CN)_6/K_4Fe(CN)_6$ (1:1) containing 0.1 M KCl. (a–g): Ppy–Co_3O_4/IL-CPE, Co_3O_4/IL-CPE, Ppy–Co_3O_4/IL/Hb-CPE, IL–CPE, Ppy–Co_3O_4/IL/GOD-CPE, Co_3O_4–CPE and CPE; (a′–c′): 40% Ppy–Co_3O_4/CPE, 20% Ppy–Co_3O_4/CPE and 5% Ppy–Co_3O_4/CPE.

−0.320 V for Hb, and −0.398 V and −0.517 V with the formal potential −0.457 V for GOD, which were similar to that of the Hb/GOD on the other nanomaterial modified electrodes previously reported [26,27], indicating that the direct electron transfer of Hb/GOD was achieved through the incorporation into Ppy–Co_3O_4/IL composite film. When weight percentage of pyrrole monomer added was up to 40% (Fig. 5A-e and Fig. 5B-e), the constant current values were almost maintained, but the electrodes' stability reduced. Apparently, the Ppy deposited on the Co_3O_4 surface plays a crucial role in the DET. Considering the results of SEM, EIS and CVs, the 20% Ppy–Co_3O_4 is appropriate for the immobilization of Hb/GOD.

The enhanced redox peak currents and low ΔE_p value indicated that a larger amount of Hb or GOD was immobilized by the interaction between the Hb/GOD and the electrode. The above results may be attributed to the synergistic effect of Ppy–Co_3O_4 hybrid material and IL. It is believed that the Ppy–Co_3O_4 hybrid material with loose structure could provide large specific surface area as well as electrostatic interactions to increase the loading amount of Hb/GOD, and act as electron-transfer mediators to enhance the current response of Hb/GOD electrode for its good conductivity and more active sites. Meanwhile, IL with good dispersion and conductivity can form a thin and sealed membrane to make the Hb/GOD molecules encapsulated in the composite film, aiding in the prevention of the denaturation and leakage of Hb/GOD, and enhancing the electron conductivity. Thus, the composite film could provide suitable microenvironment for the immobilization of the Hb/GOD and promotes the electron transfer between protein/enzyme and electrodes surface.

3.5. The kinetic parameters

CVs of Ppy–Co_3O_4/IL/Hb-CPE and Ppy–Co_3O_4/IL/GOD-CPE at different scan rates are shown in Fig. 6A and B, respectively. As seen in inset of

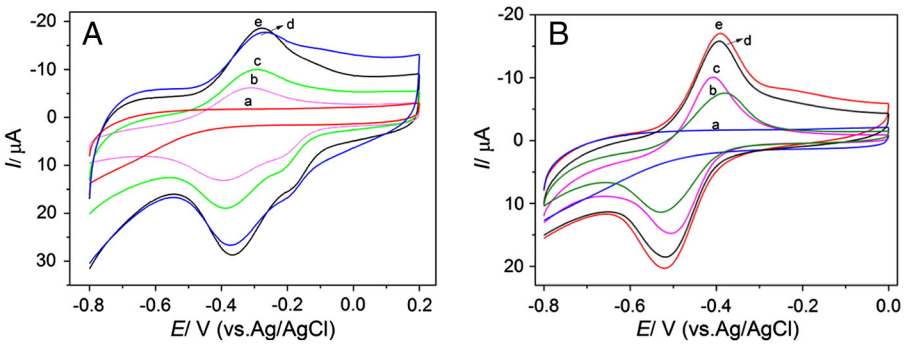

Fig. 5. (A) Cyclic voltammograms of (a) 20% Ppy–Co_3O_4/IL/CPE, (b) Co_3O_4/IL/Hb-CPE, (c) 5% Ppy–Co_3O_4/IL/Hb-CPE, (d) 20% Ppy–Co_3O_4/IL/Hb-CPE and (e) 40% Ppy–Co_3O_4/IL/Hb-CPE (B) Cyclic voltammograms of (a) 20% Ppy–Co_3O_4/IL/CPE, (b) Co_3O_4/IL/GOD-CPE, (c) 5% Ppy–Co_3O_4/IL/GOD-CPE, (d) 20% Ppy–Co_3O_4/IL/GOD-CPE and (e) 40% Ppy–Co_3O_4/IL/GOD-CPE in 0.1 M pH 7.0 PBS at a scan rate of 0.1 V s^{-1}.

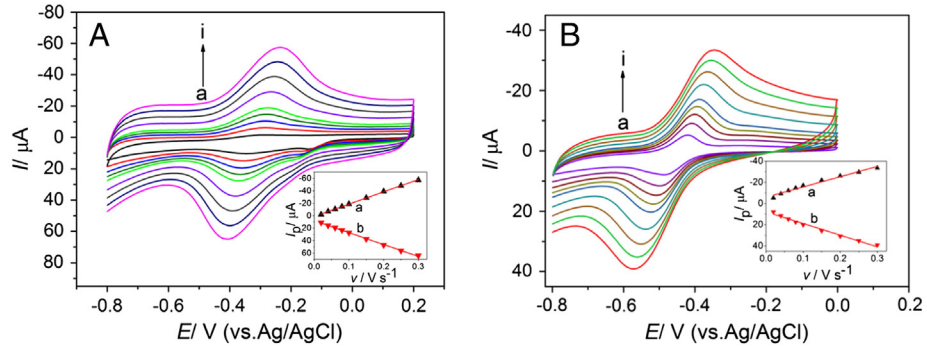

Fig. 6. (A) Cyclic voltammograms of 20% Ppy–Co_3O_4/IL/Hb-CPE (B) 20% Ppy–Co_3O_4/IL/GOD-CPE in 0.1 M pH 7.0 PBS with scan rates from 0.02 to 0.30 V s^{-1} (a–i). Insets show the plots of anodic (a) and cathodic (b) peak currents vs. scan rates.

Fig. 6A and B, the cathodic and anodic peak currents increased linearly with the increase of scan rate from 0.02 to 0.30 V s^{-1}, and the equations of calibration curves were described as: $i_{p,c}/\mu A = 190.19(\pm 2.6)\ v/\text{mV s}^{-1} + 8.24(\pm 0.42)/\mu A$; $i_{p,a}/\mu A = -197.59(\pm 2.1)\ v/\text{mV s}^{-1} + 1.26(\pm 0.34)/\mu A$ for Ppy–Co_3O_4/IL/Hb-CPE, and $i_{p,c}/\mu A = 109.29(\pm 5.0)\ v/\text{mV s}^{-1} + 7.93(\pm 0.81)/\mu A$; $i_{p,a}/\mu A = -96.86(\pm 5.4)v/\text{mVs}^{-1} - 5.93(\pm 0.89)/\mu A$ for Ppy–Co_3O_4/IL/GOD-CPE, suggesting the electrochemical reactions of the two modified electrodes were all surface-controlled process [28,29]. For a surface-controlled process, the integration of reduction peaks gives nearly constant charge (Q) at different scan rates. The average surface coverage (Γ^*) of the electroactive Hb/GOD on the modified electrodes was estimated at a slow scan rate according to Faraday's law:

$$Q = nAF\Gamma* \quad (1)$$

where Q is the charge involved in the reaction, n is the number of electron transferred, F is Faraday's constant and A is surface area of electrode. As shown in Table 1, the Γ^* values were higher than that of Hb in PHD/MWNTs composite [26] and GOD in CdS nanoparticles [30]. Furthermore, the heterogeneous electron transfer rate constant (k_s) and the transfer coefficient (α) between Hb/GOD modified electrodes have been estimated by the following Laviron equation [31]:

$$E_{p,a} = E^{0'} + RT\ \ln v/(1-\alpha)nF \quad (2)$$

$$E_{p,c} = E^{0'} - RT\ \ln v/\alpha nF \quad (3)$$

$$\log k_s = \alpha \log(1-\alpha) + (1-\alpha)\log\alpha - \log(RT/nFv) - (1-\alpha)\alpha nF\Delta E_p/2.3RT \quad (4)$$

where v is the scan rate, ΔE_p is the peak to peak potential separation. R, T and F are symbols that have conventional meanings.

These k_s were larger than Hb modified Fe_3O_4@Au/CS [32] and GOD modified GQD [33], which indicated that the Hb/GOD immobilized into Ppy–Co_3O_4/IL composite film achieved a faster electron transfer. The larger k_s value shows that the electron shuttling between redox active sites of Hb/GOD and the electrode surface is faster in Ppy–Co_3O_4/IL-CPE. This could be attributed to the high conductivity of the Ppy–Co_3O_4/IL hybrid material.

Table 1
The electrochemical parameters of different composite film.

Composite film	$\Gamma^*(10^{-9}$ M $cm^{-1})$	k_s (s^{-1})	α	Reference
PHD/MWNTs/Hb	0.47	1.2	–	[26]
Fe_3O_4@Au/CS/Hb	0.014	1.03	0.41	[32]
Ppy–Co_3O_4/IL/Hb	4.09	1.71	0.56	This work
CdS nanoparticles/GOD	0.0154	–	–	[30]
Gox–GQD	1.8	1.12	0.48	[33]
Ppy–Co_3O_4/IL/GOD	1.59	1.67	0.49	This work

3.6. The stability and reproducibility of modified electrodes

The stability and reproducibility of Ppy–Co_3O_4/IL/Hb-CPE and Ppy–Co_3O_4/IL/GOD-CPE were investigated by CV. After several initial scans, the cyclic voltammograms kept nearly constant for 100 cycles. When the two electrodes were not in use, they were stored at 4 °C in pH 7.0 PBS for 4 weeks. After 2 weeks, 92% and 91% of the current responses were retained for Ppy–Co_3O_4/IL/Hb-CPE and Ppy–Co_3O_4/IL/GOD-CPE, respectively, while 84% and 83% were retained after 4 weeks. Meantime, the reproducibility of Ppy–Co_3O_4/IL/Hb-CPE and Ppy–Co_3O_4/IL/GOD-CPE was investigated by comparing the response currents of six modified electrodes fabricated at the same time and the RSD was 3.5% and 3.8% in PBS, respectively. These studies suggested the two modified electrodes had good stability and reproducibility, and could be potentially used for the construction of biosensors.

3.7. Amperometric response of the biosensors

Fig. 7 shows the amperometric current-time curve obtained at 20% Ppy–Co_3O_4/IL/Hb-CPE upon sequential addition of an aliquot of H_2O_2 into a continuously stirred PBS (pH 7.0) at regular intervals of 50 s. The applied potential was hold at −0.35 V. For every addition of H_2O_2, well defined and stable amperometric response was observed; within 7 s it reached a level of 95% of the steady-state current. The response currents were increased linearly with the concentration of H_2O_2 in the

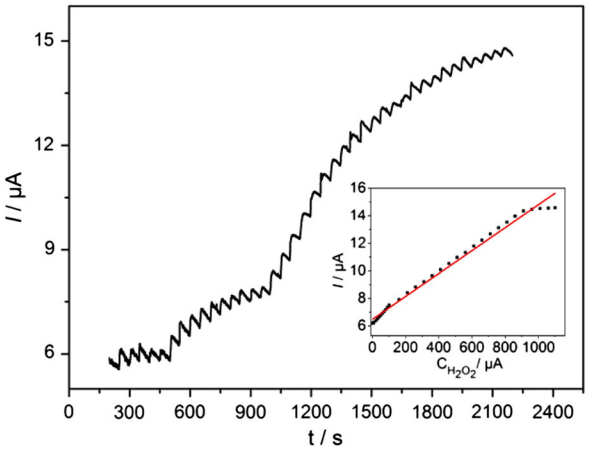

Fig. 7. Amperometric current-time response curves of 20% Ppy–Co_3O_4/IL/Hb-CPE upon successive addition of H_2O_2 into pH 7.0 PBS solution. Applied potential: −0.35 V. Inset: calibration curve of steady-state currents vs. H_2O_2 concentration at 20% Ppy–Co_3O_4/IL/Hb-CPE.

range 2.0 μM and 910 μM (inset, Fig. 7). The respective linear regression equation expressed as $I_p/\mu A = 0.00831(\pm 0.000155)c[H_2O_2]$ (μM) + 6.48(±0.0843) (R = 0.997). Detection limit (LOD) was calculated to be 0.71 μM with a signal-to-noise ratio of 3. When these results are compared with those from previous work, which involved the analysis of H_2O_2 [34,35], the performance of the novel biosensor shows a significant improvement for both linear ranges and the LOD.

The apparent Michaelis–Menten constant (K_m), which gives an indication of the enzyme substrate kinetics for the biosensor, can be calculated from the electrochemical version of the Lineweaver–Burk plot [36]

$$1/I_{ss} = 1/I_{max} + K_m/I_{max} \cdot 1/c. \quad (5)$$

Here I_{ss} is the steady-state current after the addition of substrate, I_{max} is the maximum current measured under saturated substrate condition, and C is the bulk concentration of the substrate. The K_m value was determined by analysis of the slope and intercept for the plot of the reciprocals of the steady-state current versus H_2O_2 concentration. The K_m value for the designed biosensor was found to be 0.53 mM, which is much smaller than that reported earlier [37,38]. Therefore, the immobilized Hb in 20% Ppy–Co_3O_4/IL/Hb composite possesses higher enzymatic activity, and the proposed electrode exhibits a high affinity for H_2O_2.

The probable reason for this fascinating electrocatalytic behavior of the nanobiocomposite could be due to the perfect combination of exceptional properties of 20% Ppy–Co_3O_4 hybrid, good electroconductivity property of IL and presence of large amount of electroactive Hb.

4. Conclusion

The sensing platform based on the Ppy–Co_3O_4 hybrid material with IL was demonstrated to be effective in developing protein/enzyme biosensors. This platform could endow a favorable microenvironment for loading of Hb/GOD, keeping their bioactivities and accelerating direct electron transfer of immobilized Hb/GOD on the electrode surface, and Ppy content has significant effect on DET of Hb/GOD. It is expected that its design idea may potentially be promising for immobilization and the DET of other proteins/enzymes.

Acknowledgment

The authors appreciate the support from the National Natural Science Foundation of China (No. 50830303), the Projects in the National Science & Technology (No. 2012BAC04B02) and the Overall Innovation Project of Science & Technology in Shaanxi Province (No. 2011KTCG03-07).

References

[1] C. Leger, P. Bertrand, Direct electrochemistry of redox enzymes as a tool for mechanistic studies, Chem. Rev. 108 (2008) 2379–2438.
[2] H.U. Lee, Y. Yoo, T.L. Khnagvasuren, Y.S. Song, C. Park, J. Kim, S.W. Kim, Enzymatic fuel cells based on electrodeposited graphite oxide/cobalt hydroxide/chitosan composite-enzymeelectrode, Biosens. Bioelectron. 42 (2013) 342–348.
[3] S.Y. Dong, N. Li, G.C. Suo, T.L. Huang, Inorganic/organic doped carbon aerogels as new biosensing materials for the detection of hydrogen peroxide, Anal. Chem. 85 (2013) 11739–11746.
[4] B. Vnnikishnan, S. Palanisary, S.M. Chen, A simple electrochemical approach to fabricate a glucose biosensor based on grapheme-glucose oxidase biocomposite, Biosens. Bioelectron. 39 (2013) 70–75.
[5] S.L. Zhao, X.W. Ji, P.T. Lin, Y.M. Liu, A gold nanoparticle-mediated enzyme bioreactor for inhibitor screening by capillary electrophoresis, Anal. Biochem. 411 (2011) 88–93.
[6] A.A. Saei, J.E.N. Dolatabadic, P.N. Marandi, A. Abhan, M. de la. Guaroti, Electrochemical biosensors for glucose based on metal nanoparticles, TrAC Trend, Anal. Chem. 42 (2013) 216–227.
[7] S.Y. Dong, P.H. Zhang, H. Liu, N. Li, T.L. Huang, Direct electrochemistry and electrocatalysis of hemoglobin in composite film based on ionic liquid and NiO microspheres with different morphologies, Biosens. Bioelectron. 26 (2011) 4082–4087.
[8] W. Grosse, J. Champavet, S. Gambhir, G.G. Wallale, S.E. Moulton, Aqueous dispersions of reduced graphene oxide and multi wall carbon nanotubes for enhanced glucose oxidase bioelectrode performance, Carbon 61 (2013) 467–475.
[9] W. Sun, Y.Q. Guo, X.M. Ju, Y.Y. Zhang, X.Z. Wang, Z.F. Sun, Direct electrochemistry of hemoglobin on graphene and titanium dioxide nanorods composite modified electrode and itselectrocatalysis, Biosens. Bioelectron. 42 (2013) 207–213.
[10] L.X. Wang, J. Bai, X.J. Bo, X.L. Zhang, L.P. Guo, A novel glucose sensor based on ordered mesoporous carbon–Au nanoparticles nanocomposites, Talanta 83 (2011) 1386–1391.
[11] C.C. Xiang, M. Li, M.G. Zhi, A. Manirannan, N.Q. Wu, A reduced graphene oxide/Co_3O_4 composite for supercapacitor electrode, J. Power. Sources 226 (2013) 65–70.
[12] Y.Q. Fan, N. Zhang, L.Y. Zhang, H.B. Shao, J.M. Wang, J.Q. Zhang, C. Cao, Co_3O_4-coated TiO_2 nanotube composites synthesized through photo-deposition strategy with enhanced performance for lithium-ion batteries, Electrochim. Acta 94 (2013) 285–293.
[13] V.R. Mate, M. Shiral, C.V. Rode, Heterogeneous Co_3O_4 catalyst for selective oxidation of aqueous veratryl alcohol using molecular oxygen, Catal. Commun. 33 (2013) 66–69.
[14] A.A. Ensafi, M.J. Asl, B. Rezae, A novel enzyme-free amperometric sensor for hydrogen peroxide based on Nafion/exfoliated graphene oxide–Co_3O_4 nanocomposite, Talanta 103 (2013) 322–329.
[15] X.B. Lu, G. F. Z., J.H. Li, Hemoglobin entrapped within a layered spongy Co3O4 based nanocomposite featuring direct electron transfer and peroxidase activity, J. Mater. Chem. 17 (2007) 1427–1432.
[16] Y. Ding, Y. Wang, L. Su, M. Bellagamba, H. Zhang, Y. Lei, Electrospun Co_3O_4 nanofibers for sensitive and selective glucose detection, Biosens. Bioelectron. 26 (2010) 542–548.
[17] X.W. Qi, H.W. Gao, Y.Y. Zhang, X.Z. Wang, Y. Chen, W. Sun, Electrochemical DNA biosensor with chitosan–Co_3O_4 nanorod–graphene composite for the sensitive detection of *Staphylococcus aureus* nuc gene sequence, Bioelectrochemistry 88 (2012) 42–47.
[18] F. Valentini, L.G. Fernadez, E. Tamburri, G. Palleschi, Single walled carbon nanotubes/polypyrrole–GOx composite films to modify gold microelectrodes for glucose biosensors: study of the extended linearity, Biosens. Bioelectron. 43 (2013) 75–78.
[19] I.M. Apetrei, C. Apetrei, Amperometric biosensor based on polypyrrole and tyrosinase for the detection of tyramine in food samples, Sens. Actua. B 178 (2013) 40–46.
[20] M.J.A. Shiddiky, A.A.J. Torriero, Application of ionic liquids in electrochemical sensing systems, Biosens. Bioelectron. 26 (2011) 1775–1787.
[21] H.G. Liu, Y. Liu, J.H. Li, Ionic liquids in surface electrochemistry, Phys. Chem. Chem. Phys. 12 (2010) 1685–1697.
[22] F.F. Tao, C.L. Gao, Z.H. Wen, Q. Wang, J.H. Li, Z. Xu, Cobalt oxide hollow microspheres with micro- and nano-scale composite structure: fabrication and electrochemical performance, J. Solid State Chem. 182 (2009) 1055–1060.
[23] S.Y. Dong, N. Li, T.L. Huang, H.S. Tang, J.B. Zheng, Myoglobin immobilized on LaF_3 doped CeO_2 and ionic liquid composite film for nitrite biosensor, Sens. Actua. B 173 (2012) 704–709.
[24] P. George, G. Hanania, The ionization of acidic metmyoglobin, Biochemistry 55 (1953) 236–243.
[25] S.Q. Liu, Z.H. Dai, H.Y. Chen, H.X. Ju, Immobilization of hemoglobin on zirconium dioxide nanoparticles for preparation of a novel hydrogen peroxide biosensor, Biosens. Bioelectron. 19 (2004) 963–969.
[26] Z. Wang, J. Yi, S. Yang, Direct electrochemistry and electrocatalysis of hemoglobin incorporated in composite film based on diblock weak polyelectrolyte PHAEMA-b-PDMAEMA and multi-walled carbon nanotubes, Sens. Actua. B 176 (2013) 211–216.
[27] C.C. Qiu, X. Wang, X.Y. Liu, S.F. Hou, H.Y. Ma, Direct electrochemistry of glucose oxidase immobilized on nanostructured gold thin films and its application to bioelectrochemical glucose sensor, Electrochim. Acta 67 (2012) 140–146.
[28] J.F. Rusling, A.E.F. Nassar, Enhanced electron-transfer for myoglobin in surfactant films on electrodes, J. Am. Chem. Soc. 115 (1993) 11891–11897.
[29] R. Cao, J. Zheng, Amine-terminated ionic liquid functionalized carbon nanotube-gold nanoparticles for investigating the direct electron transfer of glucose oxidase, Electrochem. Commun. 11 (2009) 608–611.
[30] Y.X. Huang, W.J. Zhang, H. Xiao, G.X. Li, An electrochemical investigation of glucose oxidase at a CdS nanoparticles modified electrode, Biosens. Bioelectron. 21 (2005) 817–821.
[31] E. Laviron, General expression of the linear potential sweep voltammogram in the case of diffusionless electrochemical systems, J. Electroanal. Chem. 101 (1979) 19–28.
[32] Y. Liu, T. Han, C. Chen, N. Bao, C.M. Yu, H.Y. Gu, A novel platform of hemoglobin on core-shell structurally Fe_3O_4@Au nanoparticles and its direct electrochemistry, Electrochim. Acta 56 (2011) 3238–3247.
[33] R. Habib, M.R. Rahim, Graphene quantum dots as a new substrate for immobilization and direct electrochemistry of glucose oxidase: application to sensitive glucose determination, Biosens. Bioelectron. 41 (2013) 498–504.
[34] D. Shan, S.X. Wang, H.G. Xue, S. Cosnier, Direct electrochemistry and electrocatalysis of hemoglobin entrapped in composite matrix based on chitosan and $CaCO_3$ nanoparticles, Electrochem. Commun. 9 (2007) 529–534.
[35] X. Xu, J. Zhang, F. Guo, W. Zheng, H. Zhou, B. Wang, Y. Zheng, Y. Wang, Y. Cheng, X. Lou, A novel amperometric hydrogen peroxide biosensor based on immobilized Hb in Pluronic P123-nanographene platelets composite, Colloids Surf. B Biointerfaces 84 (2011) 427–432.
[36] R.A. Kamin, G.S. Wilson, Rotating ring-disk enzyme electrode for biocatalysis kinetic studies and characterization of the immobilized enzyme layer, Anal. Chem. 52 (1980) 1198–1205.
[37] J.H. Shen, X.L. Yang, Y.H. Zhu, H.G. Kang, H.M. Cao, C.Z. Li, Gold-coated silica-fiber hybrid materials for application in a novel hydrogen peroxide biosensor, Biosens. Bioelectron. 34 (2012) 132–136.
[38] L.L. Zhang, G.Q. Han, Y. Liu, J. Tang, W.H. Tang, Immobilizing haemoglobin on gold/graphene–chitosan nanocomposite as efficient hydrogen peroxide biosensor, Sens. Actuators B 197 (2014) 164–171

Sheying Dong is a Professor in College of Sciences at Xi'an University of Architecture and Technology. Her main research fields are electrochemical sensors.

Lei Peng is studying for a master's degree in the College of Sciences at Xi'an University of Architecture and Technology. He received her BS at Xi'an University of Architecture and Technology in 2011.

Dan Liu is studying for a master's degree in the College of Sciences at Xi'an University of Architecture and Technology. She received her BS at Xi'an University of Architecture and Technology in 2013.

Qiangxu Yang is studying for a master's degree in the in College of Sciences at Xi'an University of Architecture and Technology. He received her BS at Xi'an University of Architecture and Technology in 2013.

Tinglin Huang is a Professor at Xi'an University of Architecture and Technology. His main research fields are environmental science.